Articles

Substrate Specificity of 6-Deoxyerythronolide B Hydroxylase, a Bacterial Cytochrome P450 of Erythromycin A Biosynthesis†

John F. Andersen,‡,§ Kuniaki Tatsuta,∥ Hiroki Gunji,∥ Takashi Ishiyama,∥ and C. Richard Hutchinson*,‡,⊥

School of Pharmacy and Department of Bacteriology, University of Wisconsin, Madison, Wisconsin 53706, and Department of Applied Chemistry, Keio University, Yokohama, Japan

Received September 9, 1992; Revised Manuscript Received November 30, 1992

ABSTRACT: The 6-deoxyerythronolide B hydroxylase (EryF) is a soluble cytochrome P450 responsible for the stereospecific C-6 hydroxylation of the erythromycin precursor, 6-deoxyerythronolide B. Using the expression of the *eryF* gene in *Escherichia coli* [Andersen, J. F., & Hutchinson, C. R. (1992) *J. Bacteriol. 174,* 725–735] as the enzyme source, we examined the catalytic activity of the EryF protein toward several macrolide substrates related to 6-deoxyerythronolide B. The results of these studies were compared with measurements of the apparent dissociation constants for various substrates and with information from molecular modeling studies of the substrates and the enzyme–substrate complex. Only minor changes in the structure of 6-deoxyerythronolide B resulted in substrates with catalytic rates less than 1% of those seen with the natural substrate. Although the 9*S* epimer of 9-deoxo-9-hydroxy-6-deoxyerythronolide B was hydroxylated at a rate approximately equal to the natural substrate, the 9*R* epimer was hydroxylated at a 2-fold lower rate. Examination of molecular models revealed that the position of the 9-hydroxyl oxygen in the 9*S* epimer resembles that of the 9-oxo oxygen in the natural substrate more closely than in the 9*R* epimer. 8,8a-Deoxyoleandolide, which is identical to 6-deoxyerythronolide B except for the presence of a C-13 methyl group, and its (9*S*)-9-deoxo-9-hydroxy derivative were C-6 hydroxylated at a 4-fold lower rate than the natural substrate, and the 9-oxo form showed a substantially larger apparent dissociation constant. From these results, we postulate that the ethyl substituent at the 13-position of 6-deoxyerythronolide B is important in the affinity of the substrate for the enzyme, possibly by interacting with a hydrophobic active-site residue. This idea is supported by a molecular model of a possible enzyme–substrate complex, which reveals the presence of several residues that may interact with the substrate, including Leu76 which may be in a position to interact with the C-13 ethyl group. Interestingly, EryF has an Ala at the position corresponding to Thr252 of $P450_{cam}$. This Thr is conserved in all other cytochrome P450 enzymes and has been thought to be essential for oxygen binding and cleavage.

Oxygenation of macrolide antibiotics can occur at positions other than those resulting from incorporation of the acyl oxygen atoms in the biosynthetic precursors. In the 14-membered macrolides, oxygenation sites of this type are seen in erythromycin, oleandomycin, and lankamycin (Nakagawa & Omura, 1984). The 6-deoxyerythronolide B hydroxylase from *Saccharopolyspora erythraea* (Safiee & Hutchinson, 1987; Corcoran, 1981) is the only instance where an enzyme responsible for a specific oxygenation event has been purified. This soluble cytochrome P450 monooxygenase has been shown to be responsible for the stereospecific hydroxylation of 6-deoxyerythronolide B at the 6-position (Shafiee & Hutchinson, 1987; Corcoran, 1981). Following hydroxylation, the macrolide is conjugated with the deoxysugars mycarose and desosamine to form erythromycin D (Corcoran, 1981). The *eryF* gene encoding deoxyerythronolide B hydroxylase (EryF[1] or CYP107A1) has been cloned along with other erythromycin biosynthetic genes from the region of the erythromycin resistance gene, *ermE* (Weber et al., 1991). EryF has been expressed in *Escherichia coli,* and its function verified by in vitro assay (Andersen & Hutchinson, 1992). A second cytochrome P450, Orf405, has also been isolated from *S. erythraea* and shows no activity toward 6-deoxyerythronolide B despite being the most closely related member of the P450 superfamily to EryF (Andersen & Hutchinson, 1992).

Macrolides vary in their solution conformations and patterns of substitution, both of which could potentially affect their suitability as EryF substrates. In previous work, a 9-deoxy-9-hydroxy form of 6-deoxyerythronolide B was found to be a suitable substrate for the hydroxylase, suggesting that some

† This work was supported in part by NIH Grants GM 31529 (to C.R.H.) and RR 05659 (to Ivan Rayment) for the FPS mini-supercomputer. J.F.A. was the recipient of a fellowship from the American Foundation for Pharmaceutical Education.

* To whom reprint requests should be addressed at the School of Pharmacy, University of Wisconsin, 425 N. Charter St., Madison, WI 53706; FAX: (608)262-3134.

‡ School of Pharmacy.

§ Present address: Department of Entomology, University of Arizona, Tucson, AZ 85721.

∥ Department of Applied Chemistry.

⊥ Department of Bacteriology.

[1] Abbreviations: EryF, 6-deoxyerythronolide B hydroxylase; CD, circular dichroism; DTT, dithiothreitol; GC, gas chromatography; HPLC, high-performance liquid chromatography; NMR, nuclear magnetic resonance; PAGE, polyacrylamide gel electrophoresis; PMSF, *p*-phenylmethanesulfonyl fluoride; R_f, relative mobility; TLC, thin-layer chromatography; TMS, trimethylsilyl.

0006-2960/93/0432-1905$04.00/0

plasticity exists in the specificity of EryF (Shafiee & Hutchinson, 1987; Corcoran, 1981). In the present study, the catalytic activity of EryF with various macrolide substrates was examined to determine its substrate specificity and, thereby, its potential usefulness in the synthesis of novel macrolide structures. Using the 1.6-Å crystal structure of cytochrome $P450_{cam}$ (Poulos et al., 1987) as a template, a molecular model of EryF was constructed that is based on sequence alignments of bacterial cytochromes P450. Residues aligning with $P450_{cam}$ regions known to interact with substrate were replaced with the corresponding EryF residues, a substrate model was inserted in the active site, and the model of the enzyme–substrate complex was subjected to energy minimization. This analysis assisted the interpretation of the substrate structure–activity data for EryF and revealed potential sites for site-directed mutagenesis. Of particular interest is the fact that EryF lacks a threonine residue that corresponds to Thr252 of $P450_{cam}$. This residue is highly conserved in P450 sequences and is thought to play a crucial role in oxygen binding and cleavage (Poulos et al., 1987). In EryF, amino acid alignments show that Thr252 has been replaced by Ala245, a substitution known to reduce the hydroxylase activity of $P450_{cam}$ drastically (Imai et al., 1989).

EXPERIMENTAL PROCEDURES

Purification of Enzymes. EryF was purified from extracts of the *E. coli*(pWHM808) transformant (Andersen & Hutchinson, 1992). Erlenmeyer flasks (2 L) containing 1-L buffered 2× YT medium (Andersen & Hutchinson, 1992) with IPTG (1 mM) and ampicillin (100 μg/mL) were inoculated with 15 mL of a frozen suspension of this transformant. The cultures were grown ca. 18 h, and the cells were harvested by centrifugation (6000*g*). The cell pellet was washed with 50 mM Tris-HCl (pH 7.5) and 1 mM EDTA and recentrifuged (6000*g*). After resuspension of the cell pellet in 50 mM Tris-HCl (pH 7.5), 1 mM EDTA, and 0.2 mM DTT (buffer A) containing 0.2 mM PMSF, lysozyme (2 mg/mL) was added, and the suspension was incubated at room temperature for 30–45 min. Triton-X100 was added to the suspension to facilitate lysis, followed by $MgCl_2$ (25 mM) and a small amount of DNase I. After a 5-min incubation at room temperature, the cellular debris was removed by centrifugation at 39000*g*. Ammonium sulfate was added to the supernatant to 30% of saturation, followed by 30 min of stirring and centrifugation at 39000*g*. To the resulting supernatant, solid ammonium sulfate was again added to 80% of saturation, and after 30 min the mixture was centrifuged at 39000*g*.

The 80% ammonium sulfate pellet was dissolved in buffer A, dialyzed against two changes of buffer A, and applied to a column of Q-Sepharose (Pharmacia). The column was eluted batchwise with 0.1, 0.2, and 1.0 M KCl in buffer A (approximately 100 mL each). Cytochrome P450 was present in only the 0.2 M fraction as indicated by the presence of the Soret absorbance of heme at 450 nm in the optical difference spectrum of the oxidized and reduced, carbon monoxide-bound P450 complex (Matsubara et al., 1976). After 2-fold dilution, the 0.2 M eluent was applied to a Mono-Q (Pharmacia) anion-exchange column and eluted with a 100–300 mM KCl gradient in buffer A. The cytochrome P450 containing fractions were pooled, concentrated in a Centricon-30 concentrator (Amicon), and applied to a Superose-6 (Pharmacia) gel filtration column. After elution with buffer A containing 100 mM KCl, the fractions were analyzed by SDS–PAGE and pooled based on the presence of the appropriate P450 band. Visible difference

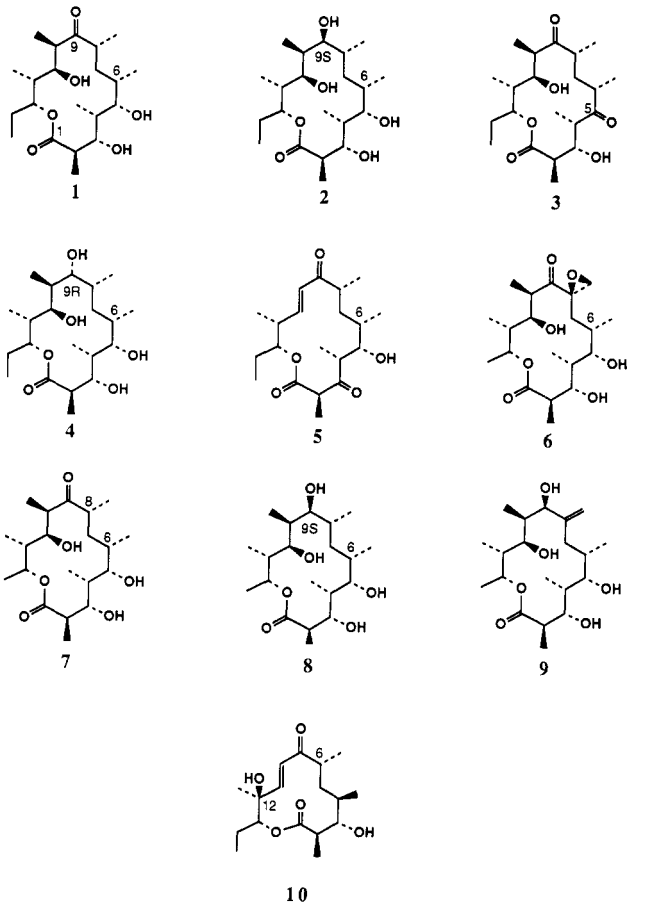

FIGURE 1: Structures of macrolides used as substrates in reactions with EryF. 6-Deoxyerythronolide B (**1**), (9*S*)-9-deoxy-9-hydroxy-6-deoxyerythronolide B (**2**), 5,6-dideoxy-5-oxoerythronolide B (**3**), (9*R*)-9-deoxy-9-hydroxy-6-deoxyerythronolide B (**4**), narbonolide (**5**), oleandolide (**6**), (8*R*)-8,8a-deoxyoleandolide (**7**), (8*R*,9*S*)-9-deoxo-9-hydroxy-8,8a-deoxyoleandolide (**8**), (9*R*)-9-deoxy-9-hydroxy-8,8a-dehydro-8,8a-deoxyoleandolide (**9**), and methynolide (**10**).

spectra (600–390 nm) of the purified EryF in its dithionite reduced, carbon monoxide-bound P450 form displayed none of the P420 form (Andersen, 1992). The P450 content was determined from the optical difference spectrum of the pooled fractions. Comparison of the total P450 content of the crude cell extract (1.8 mg/L) with that of the material obtained in the final purification step, which exhibited a single band in Coomassie-stained SDS–PAGE gels (Andersen, 1992), indicated that we obtained a 50% recovery of homogeneously pure EryF.

Substrates for Structure–Activity Studies. The structures used for experiments of substrate specificity are shown in Figure 1. Compounds **1–3** were obtained from Jim McAlpine (Abbott Laboratories, North Chicago, IL), and **1** was purified by TLC. Compound **4** was prepared by reduction of 6-deoxyerythronolide B as described previously (Shafiee & Hutchinson, 1987) and purified by preparative TLC. The radiolabeled form of this compound, (9*R*)-[9-^{3}H]-9-deoxy-9-hydroxy-6-deoxyerythronolide B, was prepared by Shafiee and Hutchinson (1987). Compound **5** was obtained from Jaroslav Majer (Northwestern University, Evanston, IL) and was purified by silica gel HPLC using a mobile phase of $CHCl_3$/MeOH (9:1, v/v). Compounds **6–9** were prepared as previously described (Tatsuta et al., 1990). Compound **10** was prepared by hydrolysis of methymycin (obtained from Satoru Masamune, MIT) by the method of Djerassi and Zderic (1956) and purified by preparative TLC on silica gel.

Assays of Enzymatic Activity. Kinetic data were obtained with the substrate (9*R*)-[9-^{3}H]-9-deoxy-9-hydroxy-6-deoxyerythronolide B. The assay mixture contained 20 mM spinach ferredoxin, 0.25 unit of spinach ferredoxin:NADP$^+$ oxidoreductase (EC 1.18.1.2), 0.8 unit of glucose-6-phosphate dehydrogenase (EC 1.1.1.49), 1.4 mM NADP$^+$, 7.6 mM glucose 6-phosphate, and 3–4 pmol of cytochrome P450 in a final volume of 0.5 mL (Andersen & Hutchinson, 1992). The mixtures were incubated for 1 min at 30 °C, and the substrate was added in 5 μL of ethanol. Assay preparations were allowed to react for 5 min, at which time the reaction was stopped by quickly vortexing the solution with 1 mL of ethyl acetate. The aqueous mixtures were thoroughly extracted with an additional 1 mL of ethyl acetate, and the combined extracts were dried under vacuum. Reaction products were analyzed by TLC and scintillation counting as described previously (Andersen & Hutchinson, 1992).

Large-scale reactions for product isolation and characterization were performed in 2-mL volumes using the assay system described above, with a substrate concentration of 4 mM. In these instances, 3–5 nmol of cytochrome P450 was added to the reaction mix, and the reactions were allowed to proceed for 1–3 h. Reaction products from these incubations were applied to silica gel TLC plates and developed with chloroform/ethanol (9:1). The recovered substrate and product bands were scraped from the TLC plate and eluted with 20% methanol in methylene chloride, and after the solution was evaporated to dryness, the residue was dissolved in ethyl acetate and filtered through a glass frit. Recovered substrate was then used to generate additional hydroxylated product by the same method. For NMR spectroscopy, the vacuum-dried, purified reaction products were dissolved in $CDCl_3$ (100 atom%, Aldrich), and proton spectra were obtained on a Bruker AM-300 spectrometer.

To obtain rate data for nonradiolabeled substrates, a gas chromatographic analysis of reaction products was developed. Assays were run as above at a substrate concentration of 100 mM, a reaction time of 10 min, and 7–10 pmol of enzyme in a total volume of 0.5 mL. The ethyl acetate extracts containing the reaction produces were evaporated to dryness and treated with Trisil solution (Pierce Chemical). After a 30-min reaction period at room temperature, the trimethylsilyl derivatives were analyzed by gas chromatography. The analysis was performed on a Hewlett-Packard 5890A gas chromatograph equipped with a hydrogen flame ionization detector and a 30-m × 0.25-mm diameter AT-1 (Alltech) fused silica capillary column. The injector and detector temperatures were set at 275 °C, and the carrier gas was helium. The temperature program consisted of an initial hold at 100 °C for 0.5 min followed by a linear increase of 10°/min to 260 °C, with a final hold of 15 min at 260 °C. The retention times of residual substrate peaks were determined by comparison with trimethylsilylated authentic standards, and those of product peaks were determined either by comparison with authentic standards, or in instances where standards were not available, by quantitative measurement of the time course of product appearance. Peak areas were determined by integration using a Hewlett-Packard 3392A integrator.

Determination of Dissociation Constants (K_D). Binding of camphor to oxidized cytochrome $P450_{cam}$ is associated with a shift of the spin-state population of the ferric heme iron from predominantly low spin to predominantly high spin (Sligar, 1976). The change in spin state manifests itself as a shift in the spectral Soret maximum of the oxidized enzyme from near 418 nm to near 390 nm. The optical difference spectrum of bound versus unbound oxidized enzyme (type I difference spectrum) can, therefore, be used to determine the apparent K_D.

Substrates dissolved in ethanol were added to a solution (0.5 mL) of purified enzyme (3.5–4.5 μM) in 50 mM Tris-HCl (pH 7.5) containing 100 mM KCl at 25 °C. Spectral scans from 500 to 380 nm were obtained at 25 °C on a Cary 14 double beam spectrophotometer fitted with an On-Line Instruments Systems (Madison, WI) data system. Difference spectra were obtained by subtracting the spectrum of the unbound enzyme from spectra of enzyme incubated with increasing concentrations of substrate. In all cases, normal type I spectra with good isosbestic points were obtained; in particular, the spectrum of oxidized EryF bound to 100 μM **1** exhibited an essentially complete shift of the 418-nm (unbound) to 390 (bound) absorption maxima (Andersen, 1992).

Molecular Modeling of EryF and Its Substrates. The active site of the EryF enzyme was modeled on the 1.6-Å X-ray crystal structure of cytochrome $P450_{cam}$ obtained from the Brookhaven Protein Database (Poulos et al., 1987). The three-dimensional structure of the substrate 6-deoxyerythronolide B was constructed from X-ray coordinates of erythromycin A (Harris et al., 1965) obtained from J. McAlpine (Abbott Laboratories, North Chicago, IL). NMR investigations have previously demonstrated that the solution conformation of the erythronolide B and 6-deoxyerythronolide B aglycons are very similar to the macrolide portion of the erythromycin A X-ray structure (Egan et al., 1973). Amino acid residues known to lie in the active site of $P450_{cam}$ were replaced by the corresponding residues in EryF based on a sequence alignment using the GAP program of the University of Wisconsin Genetics Computer Group software package with the default settings (Deveraux et al., 1984). The substitutions were made using the program Sybyl 5.4 (Tripos Associates) on a Microvax II computer and an Evans and Sutherland PS390 graphics workstation in the University of Wisconsin Molecular Modeling Laboratory in the School of Pharmacy. The model was minimized using the molecular mechanics minimization module (min) of the program Amber 3.0 (Weiner & Kollman, 1981) run on an FPS Model 522 mini-supercomputer at the University of Wisconsin Institute for Enzyme Research.

Graphical comparisons of macrolide conformations were made using the programs Alchemy (Tripos Associates) and Chem-3D (Cambridge Scientific Products). Crystal coordinate data were obtained for erythromycin A (J. McAlpine), *p*-bromobenzoyloleandomycin (Ogura et al., 1978), *p*-bromobenzoylpikromycin (Furuhata et al., 1977), 5,6-dideoxy-3α-mycarosyl-5-oxoerythronolide B (J. McAlpine), and 5-deoxy-3α-mycarosyl-5-oxoerythronolide B (J. McAlpine) and then edited to create the aglycon structures **1**, **3**, 5-deoxy-5-oxoerythronolide B, **5**, and **6**. Conformational studies of **1** and **5** with NMR suggest that the crystal structures are quite similar to the conformations seen in solution (Harris et al., 1965; Ogura et al., 1981).

RESULTS AND DISCUSSION

Characterization of EryF. Hydroxylation of the 6-deoxyerythronolide B analog (9*R*)-[9-^{3}H]-9-deoxy-9-hydroxy-6-deoxyerythronolide B (**3**) by extracts of an *E. coli* strain expressing the *eryF* gene was found to be dependent on exogenous ferredoxin and NADP:ferredoxin oxidoreductase. Previous results with this substrate (Shafiee & Hutchinson, 1987) showed the reaction rate to be linear for greater than 10 min, so end-point hydroxylation measurements were taken

at 5 min. Values for the apparent K_m and V_{max} for the (9*R*)-[9-^{3}H]-9-deoxy-9-hydroxy-6-deoxyerythronolide B substrate were determined to be 6.1 μM and 65 min^{-1}, respectively, under conditions that gave the maximum observable rate with the artificial electron transport proteins, spinach ferredoxin and NADP:ferredoxin oxidoreductase (Corcoran, 1981; Andersen & Hutchinson, 1992). [The natural electron donors to EryF are not known, although suitable electron transport proteins have been purified from *S. erythraea* (Shafiee & Hutchinson, 1988). The gene for the FdxA ferredoxin component of these proteins has been cloned, but we do not know if it is essential for the function of EryF in vivo since *fdxA* mutants could not be isolated (Donadio & Hutchinson, 1991).] The value for the apparent K_m is similar to that seen previously (Shafiee & Hutchinson, 1987), but the value for V_{max} is larger by a factor of more than 6000 than that reported for the most active fraction of 6-deoxyerythronolide B hydroxylase (Shafiee & Hutchinson, 1987). This discrepancy can be explained by the recent finding that the EryF hydroxylase copurifies with another more abundant but totally inactive (in 6-deoxyerythonolide B hydrolase assays) cytochrome P450 from *S. erythraea* extracts (Andersen & Hutchinson, 1992).

Hydroxylation of 12- and 14-Member Macrolactones by EryF. The ability of EryF to hydroxylate a variety of 12- and 14-member macrolactones was tested in order both to determine the potential usefulness of this enzyme in the production of novel macrolides and to probe the structure of its substrate binding pocket by analysis of structure–activity relationships. The products of EryF-mediated reactions were initially examined qualitatively by TLC using 200 μM substrate and ca. 0.1 nmol of enzyme. High levels of product formation were seen only for 6-deoxyerythronolide B (**1**), (9*S*)-9-deoxo-9-hydroxy-6-deoxyerythronolide B (**2**), (9*R*)-9-deoxo-9-hydroxy-6-deoxyerythronolide B (**4**), 8,8a-deoxyoleandolide (**7**), and (8*R*,9*S*)-9-deoxo-9-hydroxy-8,8a-deoxyoleandolide (**8**). The reaction between EryF and 5,6-dideoxy-5-oxoerythronolide B (**3**) produced a detectable spot with a mobility very similar to that of erythronolide B (the product of reaction of **1** with EryF), but the quantities of this product were obviously much lower than those obtained with **1**, **2**, **4**, **7**, and **8**. This is consistent with the relative amounts of **3** and its 6-hydroxy derivative produced by a *S. erythraea* mutant (Donadio et al., 1991; Katz & Hutchinson, 1992), which hydroxylated **3** only to a small extent.

The reaction products obtained with compounds **1**, **2**, and **4** could be identified by comparison of TLC R_f and GC retention times (see below) with authentic standards. No standards were available for the products derived from the oleandolide derivatives **7** and **8**, however, so the product of an EryF-mediated reaction with compound **8** was isolated and the position of hydroxylation determined by ^{1}H NMR. Assignments for the ring protons were made based on published data for the 3,5-benzylidine derivative of **8** and 6-deoxyerythronolide B (**1**). Hydroxylation at the 6-position of **8** by EryF was indicated by the loss of the resonance at δ 2.15 ppm assigned to the C-6 proton in **8**, and the absence of coupling between the C-5 and C-6 protons was seen as a simplification of the multiplet at δ 3.98 ppm assigned to the C-5 proton. The coupling constant values reported for the 3,5-benzylidine derivative of **8** are $J_{4,5}$ = 1.0 and $J_{5,6}$ = 6.0 Hz (Tatsuta et al., 1987), while the values for **8** observed here were $J_{4,5}$ = 1.47 and $J_{5,6}$ = 6.63 Hz. In the spectrum of the hydroxylation product of **8**, only the smaller 4,5 coupling is seen. The C-8 proton resonance was concealed in the ^{1}H spectra of **8** and its enzymatic product, but hydroxylation at C-8 could be discounted based on the presence of both 8,9 and 9,10 H-H coupling in the substrate and product spectra. For the 3,5-benzylidine derivative of **8**, the published coupling constants for the C-9 proton are $J_{8,9}$ = 9.0 and $J_{9,10}$ = 3.0 Hz (Ogura et al., 1981), and those obtained for **8** in this study are $J_{8,9}$ = 9.73 and $J_{9,10}$ = 3.41 Hz. Both couplings are seen in the hydroxylation product, indicating that the C-8 proton is present. The coupling constants are also very similar to those observed for the substrate **8**.

Table I: Hydroxylation and Binding of **1** and Its Analogs by EryF

compd[a]	k_{cat}[b]	relative velocity[c]	K_D[d]	ΔG[e]
1	103.0	1.00	1.98 ● 0.26	−3.69
2	106.0	1.02	5.23 ± 0.19	−3.11
3	<1.00	<0.01	6.34 ± 0.47	−3.00
4	59.2	0.57	8.45 ± 0.74	−2.83
7	23.7	0.23	142. ± 13.	−1.15
8	26.4	0.26	ND[f]	

[a] See Figure 1 for the corresponding structures. [b] Average of two replicates (min^{-1}). [c] Velocity relative to the natural substrate **1**. [d] Dissociation constant (μM). [e] $\Delta G = RT \ln K_D$ (kcal mol^{-1}). [f] ND = not determined.

Narbonolide (**5**), oleandolide (**6**), (9*R*)-9-deoxy-9-hydroxy-8,8a-dehydro-8,8a-deoxyoleandolide (**9**), and methynolide (**10**) showed little conversion to more polar products by EryF in the TLC assay. In each case a small amount of at least one product spot could be seen on the TLC plate, but the identity of these compounds was not determined.

Relative reaction rates for the six substrates that showed significant conversion to more polar products in TLC assays were determined by GC analysis of TMS derivatives of the reaction products (Table I). The products of the reactions for substrates **1**, **2**, and **4** were identified by comparison with authentic standards (obtained from J. McAlpine), while the product peaks for **7** and **8** were determined based on the increase in peak area relative to substrate after extended incubations (1 h) with enzyme (Figure 2).

The results of the GC assays showed the natural substrate **1** and the 9-deoxy-9-hydroxy derivative **2** to give the highest rates of hydroxylation. The epimer of **2**, (9*R*)-9-deoxy-9-hydroxy-6-deoxyerythronolide B (**4**), was converted at about half the rate of the natural substrate (Table I). The oleandolide derivatives **7** and **8** were converted at about one-fourth the rate of the natural substrate (Table I), despite differing from **1** and **2** by only the length of the alkyl side chain at position 13 (Figure 1).

No obvious product peak could be detected by GC analysis of the reaction of **3** with EryF, even if the assay mixtures were left to incubate at 30 °C for 1 h. These data indicate that while hydroxylation of **3** could be detected on TLC plates in assays using large amounts of enzyme (20-fold more than in the GC assay), turnover number for this substrate must be somewhat less that 1 min^{-1} (Table I).

Substrate Binding Studies. Binding of the natural substrate, 6-deoxyerythronolide B (**1**), with EryF at a concentration of 100 μM caused a nearly complete shift of the Soret band from 418 to 390 nm. The apparent K_D for the natural substrate **1** was 2.6-fold smaller than that seen for the 9*S* epimer of 9-deoxo-9-hydroxy-6-deoxyerythronolide B (**2**), and about 4.3-fold smaller than the value seen with the 9*R* epimer (**4**) (Table I). The reduced level of enzymatic hydroxylation of the 9*R* epimer relative to the 9*S* and the apparent difference in binding of these two substrates suggest that the structure of the 9*S* epimer may more closely resemble that of the natural substrate in the active site. Conformational models of the two 9-deoxy-

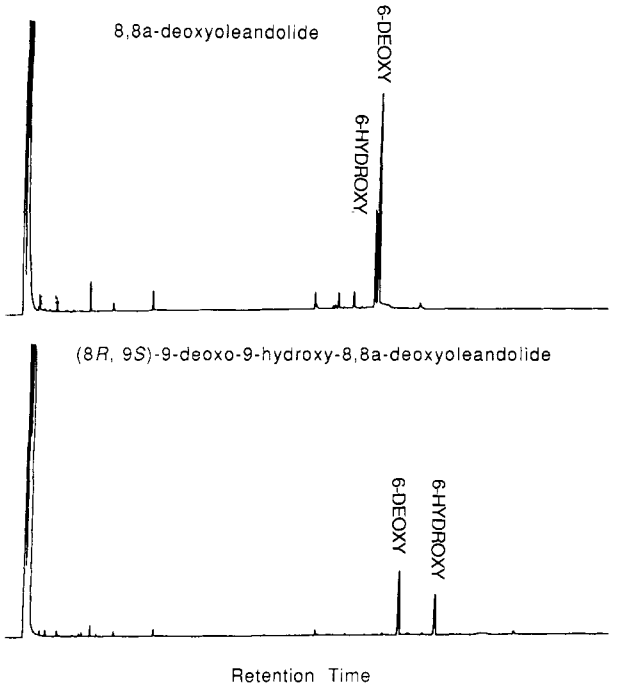

FIGURE 2: Gas chromatograms of the reaction products of 8,8a-deoxyoleandolide (**7**) and (8*R*,9*S*)-9-deoxy-9-hydroxy-8,8a-deoxyoleandolide (**8**). The chromatograms show the conversion of each substrate to hydroxylated product over the period of 1 h. Substrate concentrations were 100 mM.

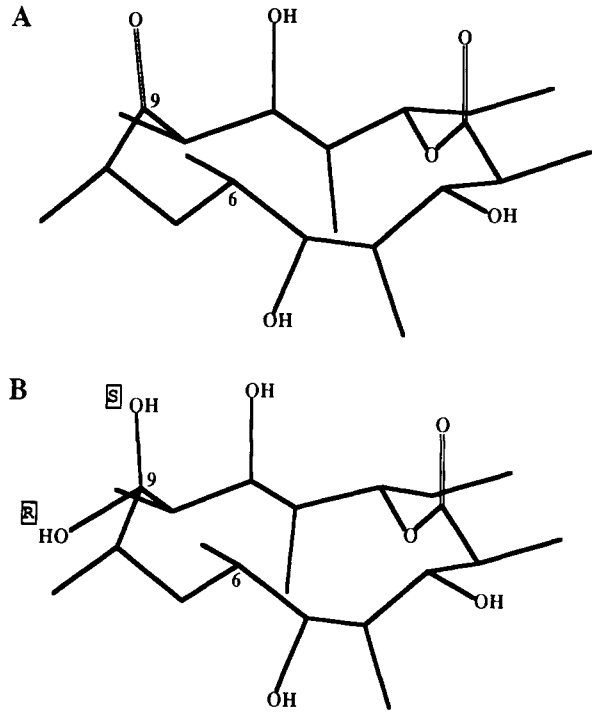

FIGURE 3: Comparison of the three-dimensional structure of **1** (A) with superimposed models of the epimers of its 9-deoxy-9-hydroxy derivatives **2** and **4** (B). The boxed letters S and R indicate the proposed positions of the C-9 oxygen in **2** and **4**, respectively. The positions of only the oxygen and hydroxyl atoms are indicated.

9-hydroxy epimers were constructed based on the crystal structure of **1** (Figure 3). The conformation around C-9 of the models agrees closely with the solution structures of the two epimers deduced from NMR data by DeMarco (1969). With the 9*S* epimer, the C-O bond at the 9 position is oriented in a very similar manner to carbonyl C-O bond in **1**, while in the 9*R* epimer the C-O bond projects outward along the plane of the macrolide ring. The similarity in the positioning of the C-9 oxygen in **1** and **2** may explain the superiority of **2** as a substrate in comparison with **4** (Figure 3).

Despite differing from **1** only in the length of the alkyl group at C-13, the apparent K_D for **7** was substantially elevated over that seen with the natural substrate, representing a loss of about 2.54 kcal mol^{-1} of binding energy (Table I). Apparently, the length of the alkyl chain has a strong influence on substrate binding, and the shortening of this chain by one carbon is at least partially responsible for the 4-fold decrease in the hydroxylation rate of **7** in comparison with **1**. The shortening of the C-13 alkyl group would not be expected to greatly alter the conformation of the macrolide structure **1**, suggesting that a specific interaction exists between the alkyl group and a hydrophobic active-site residue.

Spectral shift experiments with the 6-deoxyerythronolide B derivative **3** showed levels of binding comparable to those of substrates that are hydroxylated far more efficiently (Table I). Values for the K_D of **3** with oxidized EryF were close to those seen with **2**, which is readily converted to a hydroxylated product. Comparison of the three-dimensional models of the natural substrate **1** with a structure of **3** shows the two to be conformationally similar (Figure 4A,B). Both show a cis orientation of the C-O bonds at C-1 and C-9 and are nearly identical in the vicinity of C-6 despite the difference in oxidation state at C-5. The reason for the poor hydroxylation rate of **3** is not known, but a model of the hydroxylation product of **3** based on the crystal structure of its 3α-mycarosyl monoglycoside (Donadio et al., 1991) suggests that a major conformational change occurs when **3** is hydroxylated (Figure 5). The result of this change is that the C-9 carbonyl group is rotated nearly 90° from its position in **3** (Figure 5). NMR and CD studies have shown the major conformers of **1** and its hydroxylation product to be nearly identical (Egan et al., 1973), suggesting that no major conformational change of substrate or product would occur in the active site of EryF during the normal course of the reaction. A large difference in the stable conformation of **3** and its hydroxylation product thus may contribute significantly to the low level of hydroxylation observed with **3** in vitro and in vivo.

The weakly hydroxylated substrates **6** and **10** were tested for binding with EryF. As expected, very small shifts in the position of the Soret maximum were seen, in the presence of high (2 mM) substrate concentrations. The crystal conformation of **6** is reasonably similar to that of **1** (Figure 4C), suggesting that major conformational differences of the substrate are not responsible for the lack of binding of **6**. It is possible that a combination of the shortened alkyl side chain at position 13 (as already demonstrated for **7**) and the presence of an extra substituent at position 8 act to weaken the affinity to the point where binding is difficult to detect.

The unsaturated 14-membered macrolide narbonolide (**5**) was not tested for binding. However, it is not hydroxylated to a significant extent by EryF, and the comparison of the structural model of **5** derived from the X-ray structure of bromobenzoylpikromycin (Furuhata et al., 1977) suggests that poor hydroxylation can be attributed to a very large difference in preferred conformation between **5** and more suitable EryF substrates (Figure 4D).

In interpreting the relationships between k_{cat} and K_D for all of these substrates, we have assumed that no major alterations in the substrate and enzyme conformations take place during the initial stages of catalysis and that the rate of product release is comparable for the substrates that underwent hydroxylation. We, furthermore, have not determined if the facility of electron transport or the amount of peroxide formed,

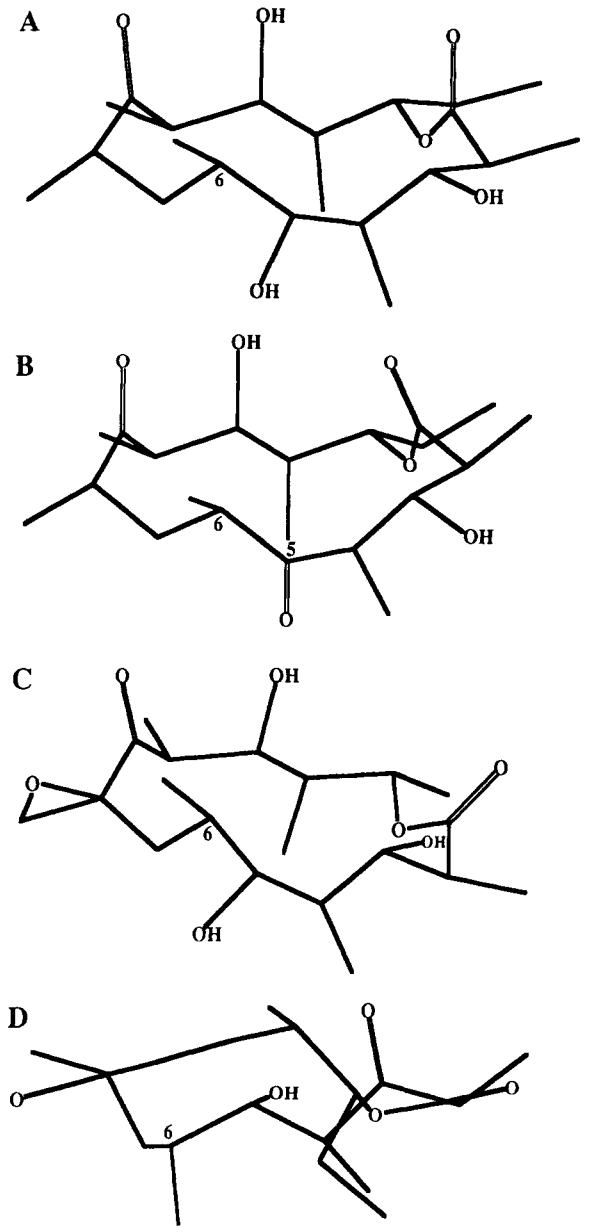

FIGURE 4: Structures of 14-membered macrolides based on crystallographic coordinates of their glycosides. (A) Structure of **1** based on crystal structure of erythromycin A. (B) Structure of **3** based on the crystal structure of 5,6-dideoxy-3α-mycarosyl-5-oxoerythronolide B (coordinate data provided by Jim McAlpine, Abbott Laboratories, North Chicago, IL). (C) Structure of **6** based on crystal data for *p*-bromobenzoyloleandomycin (Ogura et al., 1978). (D) Crystal structure of **5** based on the coordinate information for *p*-bromobenzoylpicromycin (Furuhata et al., 1977). The structures are arranged such that carbon 6 occupies the same relative position in each, and the positions of only the oxygen and hydroxyl atoms are indicated.

if any [due to decoupling of oxygen activation and substrate hydroxylation (Imai et al., 1989)], is different for different substrates. These factors might affect the hydroxylation rate data but were beyond the scope of the present investigation.

Modeling of the Active Site of EryF. Molecular modeling of the active site of EryF was performed to determine the possible positioning of the macrolide in the substrate pocket and to examine any potential contacts of the substrate with nearby amino acid residues. The 1.6-Å resolution crystal structure of cytochrome $P450_{cam}$ has proven to be a suitable template for the modeling of other P450 enzymes (Graham-Lorence et al., 1991; Laughton & Neidle, 1990; Poulos, 1991), and site directed mutagenesis studies have generally supported the idea of a common topological structure for P450 substrate

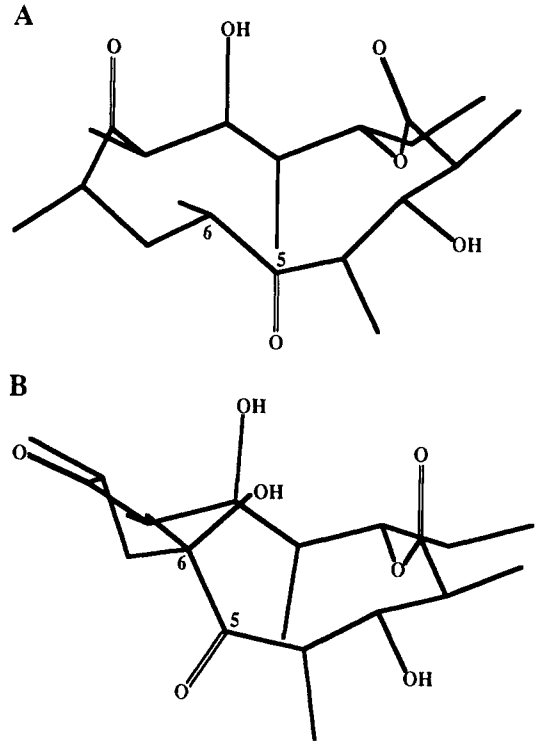

FIGURE 5: Three-dimensional structures of 5,6-dideoxy-5-oxoerythronolide B (A) and 5-deoxy-5-oxoerythronolide B (B) based on the X-ray structures of their 3α-mycarosyl monoglycosides. The positions of only the oxygen and hydroxyl atoms are indicated.

binding sites (Graham-Lorence et al., 1991). Using the Sybyl program, the active-site residues of $P450_{cam}$ were replaced by the corresponding residues in EryF as determined by amino acid alignment [with the PILEUP program (Devereux et al., 1984)] of EryF, Orf405, $P450_{cam}$, and three P450 forms from various actinomycete species (Figure 6A). EryF and $P450_{cam}$ exhibit approximately 21% positional identity, including a number of residues that are invariant in all P450 enzymes sequenced to date. Amino acid replacements were made in three areas of the $P450_{cam}$ sequence (Figure 6B), including all residues that were found to lie within 4 Å of the camphor substrate in the published crystal structure (Poulos et al., 1987). Upon replacement, the internal coordinate positions of the backbone atoms of the individual residues in $P450_{cam}$ were maintained.

The first substituted region (Figure 6C) corresponds to a portion of the distal helix I (Poulos et al., 1987) in $P450_{cam}$ which contains Thr252, a residue thought to be involved in the accommodation of molecular oxygen in the active site. Interestingly, Thr252 itself is replaced in EryF by Ala245. Inspection of published P450 sequence alignments reveals that the occurrence of this residue is essentially invariant in both prokaryotes and eukaryotes (Poulos et al., 1987) and that EryF is a very rare example of substitution at this position. All of the other actinomycete cytochromes P450 sequenced to data contain a threonine residue at this position. The validity of the alignment of Thr252 in $P450_{cam}$ and Ala245 in EryF is based on the proximity of this residue to the sequence LLAGFE244, which corresponds to the sequence in $P450_{cam}$ of LVGGLD251 (Figure 6B). In $P450_{cam}$, a hydrogen bond between the side-chain hydroxyl group of Thr252 and the carbonyl oxygen of Gly248 disrupts the normal α-helical hydrogen-bonding pattern between residues 248 and 252 (Poulos et al., 1987). This disruption results in a kink or bend in the helix around the GG dimer in the $P450_{cam}$ sequence, which is thought to form a pocket for oxygen binding. All

(A)

```
        1                                                                                                             100
  EryF} .......... ........MT t..VpDLes. ..DsFhvdwy rtYAeLREta PVTpVRFl.G qDAWLVTgYD EakAALsDlR LSSDpkkk.Y PgVEveFpAy
Orf405} .......... ........MT tgeVpDLlaF .dDaFaQdrh nrYArMRE.e PVqRIRtvnG lDAWLITRYE DvkqALlDPR iakDfgRt.q qiIEkrL.Ad
  SuaC} .........m tdTAttPqtT DApafpsnR. ..scpYQlpd gyaqlrdtpg PlhRVtLYDG RqAWvVTkhE aaRklLgDPR LSSnrtddnF PatsprFeAV
  SubC} .......... mtTAertapp DALtvpasRa .PgcpFdpap DvteAaRt.e PVTRatLWDG sscWLVTRhq DvRAvLgDPR FSaDahRtgF PFltaggreI
  ChoP} .......... ........MT qAapvtFstv .rEnYFgppa Em.qALRhka PVTRtaFaDG RpgWLVTgYs aaRAvLsDsR FtargeRe.. ..........
  CamC} mttetiqsna nlaplpPhvp EhLVfDFdmY nPsnLsagvq EaWAvLqEsn vpdlVwtRcn gghWiaTRgq liReAyeDyR hfS....sec PFIpreagea
Consen ---------- --TA--P-MT DALV-D--R- -PD-FFQ--- E-YAALRE-- PVTRVR--DG RDAWLVTRYE D-RAAL-DPR -SSD--R--F PFIE--F-A-

        101                                                                                                           200
  EryF} lgFPedvrny FatnMgtsDP PtHTRLRkLV sQEFTVRRVE aMRPRVEqIt aELLDev.gd sgvvDiVvrF AhPLPikVIC ELLGVdEkyR geFgrwSsei
Orf405} aErrPgFspd LgphMLntDP PDHTRLRkLV VkaFTaRRVE gLRPRIEqIt DDLLDrL.AG rsevDLIDEF AFPLPitVIs ELMGVeDsrR DdF..RSwtn
  SuaC} rEsPqaF... .....igLDP PEHgtrRRMt IsEFTVkRIk gMRPeVEeVv hgFLDeMlAa gptADLVsqF ALPvPsMVIC rLLGVPyaDh EfFQDaSkRL
  SubC} igtnPtF... .....LRMDd PEHaRLRRMl taDFiVkkVE aMRPeVqrla DDLvDrMttG rtsADLVtEF ALPLPsLVIC lLLGVPyeDh afFQERSrvL
  ChoP} ...hPav... .....pRaat lEdeRcRRLI agqFTaRRmr qLtgRtErIv rEhLDaMehm gspADLVEhF ALPvPsLVIa ELLGVPpaDR EqFQhdtlRw
  CamC} yDFiPt.... ......sMDP PEqrqFRaLa nQvvgmpvVD kLenRIqela csLiEsLrpq .gqcnFtEDY AePFPirIfm lLaGlPEeDi phLkyltdqM
Consen -EFPP-F--- ----MLRMDP PEHTRLRRLV -QEFTVRRVE --RPRVE-I- D-LLD-M-AG ---ADLVEEF ALPLP-LVIC ELLGVPE-DR E-FQ-RS-RL

        201                                                                                                           300
  EryF} lvMdPEraEq rgQAarEvVn FildLVerrR TEPGDDLlSA LIrvqdDdDG rLsaDELtSi ALvLLlAGfE asvsLIgigt YLLLtHPDQL AlvRrDPSal
Orf405} vlvdgsqpEa qAQAsvaMVE YLteLIakKR TEPGDDLltA LleAveDgD. rLsEgELiaM vFLLLVAGHE TTvNLIgncv LsLLgnPDQL AALRnDPSLl
  SuaC} v.qstDaqsa lt.ArnDLag YLdgLItQfq TEPGagLvgA LV.AdqlAnG eidrEELiSt AMLLLIAGHE TTasMtsLSv itLLDHPEQy AALRADrSLV
  SubC} ltLrstpEEv rA.AqdELlE YLarLartKR erPdDaiiSr LV.....ArG eLdDtqiatM grLLLVAGHE TTaNMtaLSt LvLLrnPDQL ArLRAEPaLV
  ChoP} ggFgrstEEv te.AfvsLgg qLqrLVrlKR TEPGDDLlSg LI.A...ADp aLtDEELaSi AFLLLVAGHg TTahqIaLga FLLLEHPDQL AALRADPaLt
  CamC} t..rPDgsmt fAeAkeaLyD YLipiIeQrR qkPGtDaiS. iVangqvngr pitsDEakrM cgLLLVgGlD TvvNflsFSm eFLaksPEhr qeLierPerI
Consen ----PD-EE- -AQA--ELVE YL--LI-QKR TEPGDDL-SA LV-A--DADG -L-D-EL-SM AFLLLVAGHE TT-N-I-LS- LLLL-HPDQL AALRADPSLV
                                                                                                 Δ

        301                                                                                                           400
  EryF} PnAVEEiLRY iAp.petTTR fAaEEVEIGG VaIpqystVL VAnGAANRDp kqFpDPhrFD VTRDtRGHLs FGqGIHfCMG rPLAkLEgeV ALrALfgRFP
Orf405} PGAIEEtLRY eSpVanGTfR htaEaVrfGd VvIpeGElVw VAlGAANRDg ErFEDPDrFD ITREttGHvA FGHGIHfCvG aaLARLEaqI AvgrLLeRFP
  SuaC} PGAVEELLRY LAIadiaggR VATaDIEVeG hlIrAGEGVI VvnsiANRDg tvYEDPDaLD IhRsaRhHLA FGfGVHqCLG QnLARLELeV iLnALMdRvP
  SubC} kGAVEELLRY LtIVhnGvpR IATEDVlIGG rtIaAGEGVL cmissANRDa EvFpggDdLD VaRDaRrHvA FGfGVHqCLG QPLARvELqI AietLLrRLP
  ChoP} esAVEELLRh LSVVhhGpTR aAlqDaDIeG tpVkAGEvVv VslGAANRDp arFErPDavD VTREdtGHLA FGHGmHqCLG rqLAaigLaV ALtALLgRFP
  CamC} PaAcEELLRr FSlVadG..R IlTsDyEfhG VqlkkGDqIL lpqmlsglDe renacPmhvD fsRqkvsHtt FGHGsHlCLG QhLARrEiiV tLkewLtRiP
Consen PGAVEELLRY LSIV--GTTR IATEDVEIGG V-I-AGEGVL VA-GAANRD- E-FEDPD--D VTR--RGHLA FGHG-H-CLG QPLARLEL-V AL-ALL-RFP
                            Δ                                                         Δ

        401
  EryF} aLsLgIdADD VVWRrSLLlr GIDhLPVrlD g......
Orf405} DLRMAaspDD lrWRfSvLmr GlEkLPVrpg a......
  SuaC} tLRLAVPvEq lVLRpgttIq GVneLPVtW. .......
  SubC} DLRLAVPhEE IpFRgdMaIy GVhsLPIaW. .......
  ChoP} hLRLAcPAaE IpLRhdMqVy GaDrLPVaW. .......
  CamC} DFsiApgAq. .IqhkSgiVs GVqaLPlvWD pattkav
Consen DLRLAVPA-- IVLR-SML-- GVD-LPV-WD -------
```

(B)

```
EryF    DLRLSSDPKKK.YPGVEVEFPAYLGF
Orf405  DPRIAKDFGRT.QQIIEKRL.ADAER
SU1     DPRLSSNRTDDNFPATSPRFEAVRES
SU2     DPRFSADAHRTGFPFLTAGGREIIGT
Cam     DYRHFS....SECPFIPREAGEAYDF 98

EryF    LTSIALVLLLAGFEASVSLIGIGTY
Orf405  LIAMVFLLLVAGHETTVNLIGNCVL
SU1     LISTAMLLLIAGHETTASMTSLSVI
SU2     IATMGRLLLVAGHETTANMTALSTL
Cam     AKRMCGLLLVGGLDTVVNFLSFSME 262

EryF    AVEEILRYIAP.PETTTR
Orf405  AIEETLRYESPVANGTFR
SU1     AVEELLRYLAIADIAGGR
SU2     AVEELLRHLSVVHHGPTR
Cam     ACEELLRRFSLVADG..R 299
```

(C)

```
 61 PKKKYPGVEVEFPAYLGF 78 EryF
 81 FSSECPFIPREAGEAYDF 98 Cam

231 LTSIALVLLLAGFEASVSLIGIG 253 EryF
238 AKRMCGLLLVGGLDTVVNFLSFS 260 Cam

287 PPETTT 294 EryF
293 SLVADG 298 Cam
```

FIGURE 6: Alignment and modeling of the EryF active site. (A) Alignment of EryF with the actinomycete P450 sequences Orf405 (Andersen & Hutchinson, 1992), SU1 (Omer et al., 1990), SU2 (Omer et al., 1990), and ChoP (Horii et al., 1990) and the $P450_{cam}$ sequence by the PILEUP program (Devereux et al., 1984), which uses the algorithm of Needleman and Wunsch (1970). Gaps are indicated by dotted lines and the "Consen" line displays a capital letter whenever two or more identical residues are present in a column. The locations of three highly conserved residues are indicated by a Δ. (B) Regions of five of these aligned sequences corresponding to the modeled region of EryF. (C) The sequence substitutions made with the Sybyl program, with each residue of $P450_{cam}$ being substituted by the EryF residue shown directly above it.

known P450 sequences contain either a GG or AG dimer at this position, and the alignment shows a high degree of similarity in this region of EryF with other actinomycete P450 sequences (Figure 6A).

The second $P450_{cam}$ sequence in which amino acid replacements were made (Figure 6C) includes a portion of sheet β3 and the loop connecting sheet β3 to helix K directly N-terminal to Arg299 (Poulos et al., 1987). This arginine residue is highly conserved and is thought to be involved in an electrostatic interaction with one of the propionate side chains of heme (Poulos et al., 1987). In $P450_{cam}$, this sequence contains Val295, a residue that interacts with the geminal dimethyl group of camphor. The third altered sequence (Figure 6C) is contained within helix B′ (Poulos et al., 1987) and surrounding residues and contains Tyr96, which interacts with the carbonyl group of camphor via a hydrogen bond. This region is highly variable in P450 sequences, making it difficult to align precisely. However, the PILEUP alignment of six

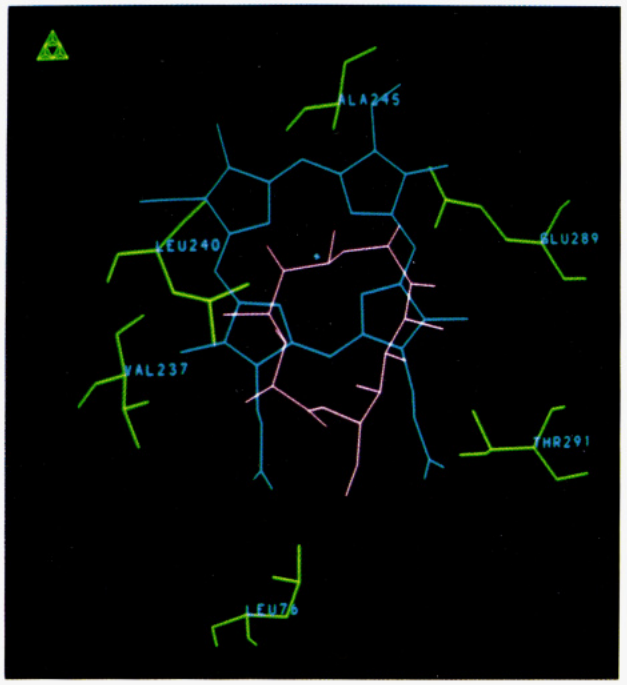

FIGURE 7: Model of the enzyme–substrate complex viewed perpendicular to the heme plane and showing residues having close contacts with the substrate. Amino acid side chains are shown in green, the heme is shown in blue, and the substrate is shown in magenta.

bacterial P450 sequences suggests that Leu76 or EryF aligns with Tyr96 of $P450_{cam}$ (Figure 6A).

The three-dimensional model of the substrate, 6-deoxyerythronolide B (**1**), was obtained from the crystal structure of erythromycin A in which coordinate information for the two deoxysugars, the C-6 hydroxyl group, and the C-12 hydroxyl group had been removed and replaced by hydrogen. The substrate model was built from a coordinate file using Sybyl and introduced into the active-site model of EryF that also contained the structure of camphor in the same relative position as is seen in $P450_{cam}$ (Poulos et al., 1987). In $P450_{cam}$, the substrate has been proposed to approach the oxygen-bound iron from the side, such that maximal interaction of the C-H bond of the substrate with the oxygen p orbitals occurs (Poulos et al., 1987). The reactive oxygen abstracts the substrate C-5 exo hydrogen atom followed by collapse of the substrate radical to form the hydroxylated product. The C-6 H bond of **1** was directed toward the heme face, such that the C-H bond was oriented similarly to the C-5 exo H bond in camphor, and C-6 of **1** was oriented to occupy the same spatial position as C-5 (the $P450_{cam}$ oxygenation site) in camphor. This rationale for substrate positioning has been used in the modeling of other P450–substrate complexes (Graham-Lorence et al., 1991; Poulos, 1991). The substrate was further positioned in the active site to occupy as little space as possible in the vicinity of Ala245 (the positional analog of Thr252 in $P450_{cam}$), which we assume to be the dioxygen binding site (Poulos et al., 1987). Taking all of these factors into account, the most likely orientation of **1** in the hypothetical active site of EryF is that shown in Figure 7.

After removal of the camphor coordinates, the EryF–substrate complex active-site model was subjected to energy minimization using the Amber 3.0 molecular mechanics minimization module (Weiner & Kollman, 1981). Only the substrate and amino acid sequence regions that were replaced in $P450_{cam}$ were included in the minimization, while all other portions of the molecule, including the heme prosthetic group, were held fixed using the belly option of the Amber minimization module. With this option the bonded interactions of the fixed regions are not included in the calculations, and only the nonbonded parameters of the fixed region influence the energy-minimized structure. Most parameters for the nonstandard residues, heme, and **1** were determined using the standard Amber force field atom types defined by Weiner et al., (1984), and partial charges were not calculated for these residues. Because of limitations in computational capability, the size of the enzyme had to be reduced. Residues were removed from the N-terminus of the protein up to Ile71 in $P450_{cam}$, and from the C-terminus to Arg364. The eliminated residues did not lie within 4 Å of the camphor substrate in $P450_{cam}$ and were not in the group determined by X-ray crystallography to be involved in heme binding (Poulos et al., 1987). Also, the helix I sequence included in the belly minimization extended only from residues 240 to 255 of $P450_{cam}$ (see Figure 6A). This stretch of residues contains all of the portion of helix I lying within 10 Å of the camphor substrate (Poulos et al., 1987). Finally, three dipeptide sequences found to lie within 10 Å of the camphor substrate, but not within 4 Å (Poulos et al., 1987), were not replaced or included in the minimization. These sequences are MT185, AK197, and IV396. The modified P450 structure was minimized by steepest descents for 50 iterations, followed by conjugate gradient minimization until the RMS gradient was less than 0.1 kcal mol^{-1} $Å^{-1}$.

The model resulting from energy minimization of the altered enzyme identifies a number of residues whose side chains project into the active site and may interact with the substrate. While specific interactions cannot be determined with certainty, the orientation chosen for the substrate macrolide suggests that Thr291 may interact with the C-11 hydroxyl group, Leu240 with the C-4 methyl group, and Val237 with the C-2 methyl group (Figure 7). The side chain of Glu289 projects into the active site in the vicinity of the C-9 carbonyl group of the substrate and would potentially be responsible for the rate difference seen with the two epimers of the 9-deoxy-9-hydroxy substrates **2** and **4**, by interfering with the positioning of the *R* epimer in the active site (Figure 7). The side chain of Leu76 lies in a favorable position for interaction with the C-13 ethyl group of the bound macrolide (Figure 7). In substrate binding studies, a large difference in binding free energy was seen between substrates **1** and **7** that differ only in the length of the alkyl substituent at position 13 (Table I). The shortened side chain would not be expected to change the conformation of **1** significantly, so the $\Delta\Delta G$ might be in large part due to loss of an interaction of the protein with the alkyl group, although the 2.54 kcal mol^{-1} difference does seem large for a hydrophobic bond. As discussed above, this portion of the P450 protein is highly variable, but based on work with other P450s, it appears to be extremely important in the determination of substrate specificity (Kronbach et al., 1991).

Perhaps the most interesting feature of the EryF structure is the replacement of Thr252 of $P450_{cam}$ by Ala245. The helical distortion caused by the hydrogen bonding of Thr252 in $P450_{cam}$ creates a space for the binding of molecular oxygen and may be involved in a regulated delivery of protons to the active site for use in the acid-catalyzed cleavage of molecular oxygen (Ragg et al., 1991). Site-directed mutagenesis studies with $P450_{cam}$ have shown that a Thr252 to Ala substitution drastically reduces substrate hydroxylation rate, while oxygen utilization is maintained at or near wild-type levels (Imai et al., 1989). Production of large amounts of hydrogen peroxide by this mutant suggested that Thr252 may play a direct role

in oxygen cleavage (Imai et al., 1989). Raag et al. (1991) have produced a 2.1-Å crystal structure of the Ala252 mutant showing that the pocket between Thr252 and Gly248 is larger than that of the wild-type enzyme and can accommodate an extra solvent molecule that may react with the oxy–heme complex in the active site to produce peroxide. In EryF, the presence of alanine at the putative oxygen binding site results in a form of P450 which is quite efficient in oxygenation reactions, showing a turnover number of greater than 100 min^{-1} with the natural substrate. It is possible that evolution has produced in EryF an alternative way to accommodate and cleave molecular oxygen while providing an environment for the stable maintenance of the oxy–heme complex. The driving force for these changes may have been the need to accommodate a bulky macrolide substrate in an orientation that would impinge on a normally structured oxygen-binding pocket. Preparation of the EryF Ala245Thr mutant and comparisons of the relative rates of hydroxylation of **1** and amounts of peroxide formation (if any) between the wild-type and mutant enzymes should sheld light on this question. Meanwhile, it is interesting to note that Orf405 and EryK (Stassi et al., 1992), two other *S. erythraea* P450 proteins that are closely related to EryF, contain a typically situated threonine residue that aligns with Thr252 of $P450_{cam}$ (Figure 6A shows Orf405 only). The Orf405 enzyme has no detectable 6-deoxyerythronolide B hydroxylase activity and shows little or no spectral shift upon incubation with **1** (Andersen, 1992). EryK, in contrast, is the C-12 hydroxylase that acts on erythromycin D, a late intermediate of erythromycin biosynthesis (Stassi et al., 1992).

ACKNOWLEDGMENT

We thank Wendell Burkholder and Joel Phillips, Entomology Department, for assistance with the gas chromatographic analyses; Ahammadunny Pathiaseril and Dan Rich for assistance with the molecular modeling; and Evelyn Went-Peinkowski for verifying the DNA sequence of the *eryF* gene. We also are grateful to Jim McApine, Jaroslav Majer, and Sat Masamune for gifts of macrolides.

REFERENCES

Andersen, J. F. (1992) Ph.D. Dissertation, University of Wisconsin—Madison.

Andersen, J. F., & Hutchinson, C. R. (1992) *J. Bacteriol. 174*, 725–735.

Corcoran, J. W. (1981) in *Antibiotics IV: Biosynthesis* (Corcoran, J. W., Ed.) pp 132–174, Springer-Verlag, New York.

DeMarco, P. V. (1969) *J. Antibiot. 52*, 327–340.

Devereux, J., Haeberli, P., & Smithies, O. (1984) *Nucleic Acids Res. 12*, 387–395.

Djerassi, C., & Zderic, J. A. (1956) *J. Am. Chem. Soc. 78*, 6390–6395.

Donadio, S., & Hutchinson, C. R. (1991) *Gene 100*, 231–235.

Donadio, S., Staver, M. J., McAlpine, J. B., Swanson, S. J., & Katz, L. (1991) *Science 252*, 675–679.

Egan, R. S., Perun, T. J., Martin, J. R., & Mitscher, L. A. (1973) *Tetrahedron 29*, 2525–2538.

Furuhata, K., Ogura, H., Harada, Y., & Iitaka, Y. (1977) *Chem. Pharm. Bull. 25*, 2385–2391.

Graham-Lorence, S., Khalil, M. W., Lorence, M. C., Mendelson, C. R., & Simpson, E. R. (1991) *J. Biol. Chem. 266*, 11939–11946.

Harris, D. R., McGeachin, S. G., & Mills, H. H. (1965) *Tetrahedron Lett.*, 679–685.

Horii, M., Ishizaki, T., Paik, S.-Y., Manome, T., & Murooka, Y. (1990) *J. Bacteriol. 172*, 3644–3653.

Imai, M., Shimada, H., Watanabe, Y., Matsushima-Hibiya, Y., Makino, R., Koga, H., Horiuchi, T., & Ishimura, Y. (1989) *Proc. Natl. Acad. Sci. U.S.A. 86*, 7823–7827.

Katz, L., & Hutchinson, C. R. (1992) *Annu. Rep. Med. Chem. 27*, 129–138.

Kronbach, T., Kemper, B., & Johnson, E. F. (1991) *Biochemistry 30*, 6097–6102.

Laughton, C. A., & Neidle, S. (1990) *Biochem. Biophys. Res. Commun. 171*, 1160–1167.

Matsubara, T., Koike, M., Touchi, A., Tochino, Y., & Sugeno, K. (1976) *Anal. Biochem. 75*, 596–603.

Nakagawa, A., & Omura, S. (1984) in *Macrolide Antibiotics* (Omura, S., Ed.) Chapter 2, Academic Press, New York.

Needleman, S. B., & Wunsch, C. D. (1970) *J. Mol. Biol. 48*, 443–453.

Ogura, H., Furuhata, K., Harada, Y., & Iitaka, Y. (1978) *J. Am. Chem. Soc. 100*, 6733–6737.

Ogura, H., Furuhata, K., Kuwano, H., & Suzuki, M. (1981) *Tetrahedron 37*, 165–173.

Omer, C. A., Lenstra, R., Litle, P. J., Dean, C., Tepperman, J. M., Leto, K. J., Romesser, J., A., & O'Keefe, D. P. (1990) *J. Bacteriol. 172*, 3335–3345.

Poulos, T. L. (1991) *Methods Enzymol. 206*, 11–31.

Poulos, T. L., Finzel, B. C., & Howard, A. J. (1987) *J. Mol. Biol. 195*, 687–700.

Raag, R., Martinis, S. A., Sligar, S. G., & Poulos, T. L. (1991) *Biochemistry 30*, 11420–11429.

Shafiee, A., & Hutchinson, C. R. (1987) *Biochemistry 26*, 6204–6210.

Shafiee, A., & Hutchinson, C. R. (1988) *J. Bacteriol. 170*, 1548–1553.

Sligar, S. G. (1976) *Biochemistry 15*, 5399–5406.

Stassi, D., Donadio, S., Staver, M. J., & Katz, L. (1992) *J. Bacteriol. 175*, 182–189.

Tatsuta, K., Kobayashi, Y., & Kinoshita, M. (1987) *J. Antibiot. 40*, 910–912.

Tatsuta, K., Gunji, H., Tajima, S., & Ishiyama, T. (1990) *J. Antibiot. 43*, 909–911.

Weber, J. M., Leung, J. O., Swanson, S. J., Idler, K. B., & McAlpine, J. B. (1991) *Science 252*, 114–117.

Weiner, P., & Kollman, P. (1981) *J. Comput. Chem. 2*, 287–295.

Weiner, S. J., Kollman, P. A., Case, D. A., Singh, U. C., Ghio, C., Alagona, G., Profeta, S., & Weiner, P. (1984) *J. Am. Chem. Soc. 106*, 765–784.